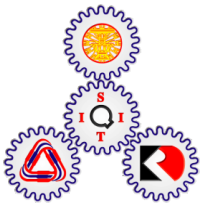

TRANSFORMATION OF REPRESENTATIVE WAVE HEIGHTS USING PARAMETRIC WAVE APPROACH

BY

NGA THANH DUONG

A THESIS SUBMITTED IN PARTIAL FULFILLMENT OF THE REQUIREMENTS FOR THE DEGREE OF MASTER OF SCIENCE (ENGINEERING AND TECHNOLOGY)

SIRINDHORN INTERNATIONAL INSTITUTE OF TECHNOLOGY

THAMMASAT UNIVERSITY

ACADEMIC YEAR 2015

TRANSFORMATION OF REPRESENTATIVE WAVE HEIGHTS USING PARAMETRIC WAVE APPROACH

BY

NGA THANH DUONG

A THESIS SUBMITTED IN PARTIAL FULFILLMENT OF THE REQUIREMENTS FOR THE DEGREE OF MASTER OF SCIENCE (ENGINEERING AND TECHNOLOGY)

SIRINDHORN INTERNATIONAL INSTITUTE OF TECHNOLOGY

THAMMASAT UNIVERSITY

ACADEMIC YEAR 2015

TRANSFORMATION OF REPRESENTATIVE WAVE HEIGHTS USING PARAMETRIC WAVE APPROACH

A Thesis Presented

By
NGA THANH DUONG

Submitted to
Sirindhorn International Institute of Technology
Thammasat University
In partial fulfillment of the requirements for the degree of
MASTER OF SCIENCE (ENGINEERING AND TECHNOLOGY)

Approved as to style and content by

Advisor and Chairperson of Thesis Committee _____

(Assoc. Prof. Winyu Rattanapitikon, D.Eng.)

Committee Member and
Chairperson of Examination Committee _____

(Prof. Tawatchai Tingsanchali, D.Eng.)

Committee Member _____

(Prof. Pruettha Nanakorn, D.Eng.)

DECEMBER 2015

Abstract

TRANSFORMATION OF REPRESENTATIVE WAVE HEIGHTS
USING PARAMETRIC WAVE APPROACH

by

NGA THANH DUONG

Bachelor of Engineering in Civil Engineering, Ho Chi Minh City University of Technology, 2013.

Wave height transformation is one of the most important parameters to study coastal engineering processes, as well as applications for coastal structures. This study researches transformation of representative wave heights, [i.e. root-mean-square wave height (H_{rms}), spectral root-mean-square wave height (H_{rmsz}), highest one-tenth wave height ($H_{1/10}$), highest one-third wave height ($H_{1/3}$), and mean wave height (H_m)] by using a parametric wave approach. The parametric wave approach is widely used for computing the transformation of H_{rms}, especially in commercial or free software. If it could be used for computing other representative wave heights, it would be useful for practical work. Nevertheless, until now, no literature has indicated that the parametric wave approach could be applicable for computing H_m, $H_{1/3}$, $H_{1/10}$, and H_{rmsz}. Hence, present study was conducted to examine the use of parametric wave models to simulate the representative wave heights transformation. Eleven parametric wave models were selected to calibrate and examine the applicability. Compiled experiment results are used for calibrating and examining the models. A new model was developed for computing transformation of H_{rms}. Unlike the existing parametric wave models, the new dissipation model was developed based on the stable energy concept. The

examination shown that present model and most of existing models (with calibrated coefficients) could be applied to compute the representative wave heights transformation. Top four models are recommended for calculating transformation of the representative wave heights.

Keywords: Representative wave heights, Energy dissipation, Parametric wave approach, Irregular wave model.

Acknowledgements

First and foremost, I wishes to express my gratefulness to my advisor, Assoc. Prof. Dr. Winyu Rattanapitikon who gave me a lot of the invaluable assistances, supports and guidance. His willingness to motivate me contributed tremendously to my thesis report.

I would like to express my gratitude to Prof. Dr. Tawatchai Tingsanchali, and Prof. Dr. Pruettha Nanakorn gave me many comments and advices to my study.

I would like to thank the previous researchers for providing the valuable experimental data used in this study.

My thanks and appreciations also go to Sirindhorn International Institute of Technology, Thammasat University, for providing me with an opportunity to study here.

Finally, I would like to thank all those who directly and indirectly helped and encouraged me all through the report.

Table of Contents

List of Tables

List of Figures

Figures **Page**

Chapter 1
Introduction

1.1 General

Nowadays, human use coastal zones for various purposes, e.g. human settlements, agriculture, industrial and commercial development, etc.. The construction of flood protection structures and coastal protection strongly influence activities in the coastal zone. An accuracy in the design of wave height is significant for a development of coastal projects, e.g. study of beach deformation and structure design. Underestimation of the wave height makes a coastal project less safe, while overestimation causes extra cost of the project. Hence, the prediction of wave height transformation is very important. So far, there are four approaches to calculate irregular wave height transformation, i.e. spectral approach, representative wave approach, parametric wave approach, and probabilistic approach. Parametric wave approach is widely used, especially in the commercial software for computing transformation of root-mean-square wave height (H_{rms}). All existing energy dissipation models of the parametric wave approach were developed from a bore concept.

1.2 Statement of study

Parametric wave approach only computes root-mean-square wave height (H_{rms}) transformation. If this approach could be used for computing other representative wave heights [i.e. root-mean-square wave height (H_{rms}), spectral root-mean-square wave height (H_{rmsz}), highest one-tenth wave height ($H_{1/10}$), highest one-third wave height ($H_{1/3}$), and mean wave height (H_m)], it would be more useful. Many experiments shown that the representative wave heights transform in similar fashion. Therefore, it may be possible to use the parametric wave approach for predicting the transformation of other representative wave heights (H_{rep}). Nevertheless, no literature researches the possibility of the applicability of parametric wave approach for computing other representative wave heights. Hence, it is necessary to study the computation of other representative wave heights transformation by using parametric wave approach.

Nowadays, the bore concept and the stable energy concept are widely used for computing the energy dissipation of regular wave breaking. Rattanapitikon et al. (2003) shown that the energy dissipation models from stable energy concept give better prediction than that of the bore concept. Because of the change of beach profiles, the models for computing wave height transformation should not be complex to update wave field to account frequently. The irregular wave is a complexity phenomenon, most of irregular energy dissipation models are developed from the empirical or semi-empirical approach. Moreover, the results of the computation are unlike with different measured data and different models. Hence, a new model may be developed with wide range of experiment condition and a large number of experimental results of previous researchers.

1.3 Objective of study

The objectives of the present study are as follows:

- To collect experimental data of representative wave heights transformation.
- To develop a new model for calculating transformation of root-mean-square wave height (H_{rms}).
- To verify the applicability of existing parametric wave models and a new model for other representative wave heights transformation (i.e. H_m , $H_{1/3}$, $H_{1/10}$, and H_{rmsz}).

1.4 Scope of study

The scopes of the present study are as follows:

- Parametric wave approach is considered in this study.
- Fourteen experiments with 1732 cases are compiled for computation.
- Eleven existing models of parametric wave approach are collected to examine and extend for calculating representative wave heights transformation.

Chapter 2
Literature Review

2.1 Breaker wave height

Waves in nature are irregular waves, the broken wave is the complex mechanism. Hence, it is difficult to determine height and position of breaking wave. Breaker wave height is an important parameter in study, as well as practical work. Hence, the predictions of the breaker heights are very significant. Some different formulas of breaker wave height were proposed by previous researchers. A brief reviews of some existing formulas used in parametric wave approach is shown below.

a) Miche (1944) proposed that the maximum height of regular waves in finite water depth is determined based on the semi-theoretical breaking criterion. The function of the ratio of water depth and wave length is the limiting wave steepness.

b) Goda (1970) re-analyzed various laboratory data on the breaker height obtained by several researchers and proposed a breaker wave height formula. The formula is used for non-uniformly sloping beaches in natural beaches.

c) Thornton and Guza (1983) proposed a simple formula of the breaker wave height. Wave height strongly depends on water depth. The formula was developed based on experimental data at Torrey Pines Beach, California.

d) Battjes and Stive (1985), based on compiled data with variety of wave conditions and bottom profiles, proposed a formula for calculating breaker wave height of irregular wave. The formula of Miche (1944) was modified by adding the term of deep-water steepness.

e) Ruessink et al. (2003) modified Miche (1944)'s the breaker wave height formula. Based on data points at Duck, Egmond and Terschelling, they proposed that the free parameter of the breaker wave height formula depends on the wave number and the water depth.

f) Apotsos et al. (2008), based on six experiments, modified Thornton and Guza (1983)'s the breaker wave height formula. The free parameter of the breaker wave height formula was proposed as a function of deep-water wave height.

2.2 Regular wave models

As waves start to break, their energy is dissipated from the breaking point to shoreline. For parametric wave approach, the energy flux balance expression is often used for determining transformation of wave height. The energy dissipation in the process of regular wave breaking (D_S) is an important term of the energy conservation equation, and it is difficult to determine this dissipation. All of existing D_S models were developed based on the stable energy concept and the bore concept that are widely used to compute the energy dissipation rate. Brief reviews of the D_S models are as follows.

a) Battjes and Janssen (1978) developed D_S model based on the bore concept to compute the energy dissipation. They reduced the dependence of the energy dissipation on the water depth by proposing that the wave height is equal to the water depth.

b) Thornton and Guza (1983) described the dissipation of breaking wave height based on bore concept. The D_S model is modified from the model of Battjes and Janssen (1978).

c) Dally et al. (1985) proposed D_S model based on stable energy concept. In this model, when the beach slope transforms from the gentle slope to horizontal bottom, wave starts to break. The breaking wave remains until on the horizontal bottom, the stable wave height is obtained. Thus, the energy dissipation rate depends on the excess energy flux relating to the stable energy flux.

d) Rattanapitikon and Shibayama (1998) used the experimental results obtained by many researchers to modify the energy dissipation model of Dally et al. (1985). They pointed out that the parametric Γ is not constant as in the study of Dally et al. (1985), and it is a function of the breaker wave height, the water depth, and the wave length.

2.3 Irregular wave models

There are four main approaches to simulate transformation of representative wave heights, i.e. representative wave approach, parametric wave approach, spectral approach, and probabilistic approach. In this study, the parametric approach is considered. For parametric wave approach, it only computes the transformation of root-

mean-square wave height (H_{rms}), and the energy flux balance is the main equation for calculating transformation of irregular wave heights. The energy dissipation of irregular waves (D_B) was proposed by many researchers. Concise reviews of some existing D_B models are shown below.

a) Battjes and Janssen (1978) developed D_B model based on the bore concept. They assumed that all breaker wave heights are the same and are the breaking wave height (H_b). This model describes fraction of breaking wave based on Rayleigh distribution truncated at the maximum wave height.

b) Thornton and Guza (1983) described the wave height transformation based on the energy conservation equation. The model was developed based on the same concept as that of Battjes and Janssen (1978). The Rayleight distribution is assumed in local probability of breaking wave (including the surf-zone) to compute the energy dissipation.

c) Battjes and Stive (1985) calibrated the coefficient of the breaker wave height formula of Battjes and Janssen (1978). Both the compiled experimental data and the field data are used for calibration. Energy dissipation equation of Battjes and Janssen (1978) is used without change.

d) Southgate and Nairn (1993) modified the D_B model of Battjes and Janssen (1978) by changing the D_S model to be the D_S model of Thornton and Guza (1983). The formula of breaker wave height of Nairn (1990) is used to determine the breaker wave height.

e) Baldock et al. (1998) proposed a new model to compute transformation of breaker wave height based on the fraction of breaking wave of the Rayleight distribution. The energy dissipation D_B was developed from the D_S model of Battjes and Janssen (1978).

f) Rattanapitikon and Shibayama (1998) proposed the new formula by modifying Battjes and Janssen (1978)'s the energy dissipation model by replacing the D_S of bore concept to the D_S of stable energy concept.

g) Ruessink et al. (2003) proposed an empirical improvement to wave height formula of Battjes and Janssen (1978) by including a new functional form. It depends

on the water depth and the wave number. The energy dissipation D_B model from Baldock et al. (1998) is completely used.

h) Alsina and Baldock (2007) modified the energy dissipation D_B of Baldock et al. (1998) by changing the D_S model of Battjes and Janssen (1978) to the D_S model of Thornton and Guza (1983). The breaker height of Battjes and Stive (1985) was completely used. The wave height is described based on the full Rayleigh distribution.

i) Janssen and Battjes (2007) used the D_B model as the model of Alsina and Baldock (2007). The breaker wave height formula of Nairn (1990) was completely used in the model.

j) Rattanapitikon and Sawanggun (2008) modified the fraction expression of the breaking waves of Battjes and Stive (1985). The percentage of the breaking wave is determined directly from the measured wave heights.

k) Apotsos et al. (2008) recalibrated a coefficient in the breaker height formula of eight existing dissipation models by broad observation from six field experiments with barred and unbarred beach condition. The coefficient is related to the deep-water wave height.

Chapter 3
Theoretical Consideration

3.1 Linear wave theory

Waves in nature are irregular waves which changes height, period, direction with time and space. It is difficult to understand clearly irregular wave phenomena because of its complexity. Therefore, to resolve this problem, some assumptions have to be set. Linear wave theory is the simplest wave theory but it is usually used in practice.

Figure 3.1 shows a water surface profile (η) and definition sketch for a wave of height (H) and length (L) propagating in constant water depth (h) in the x-z plane.

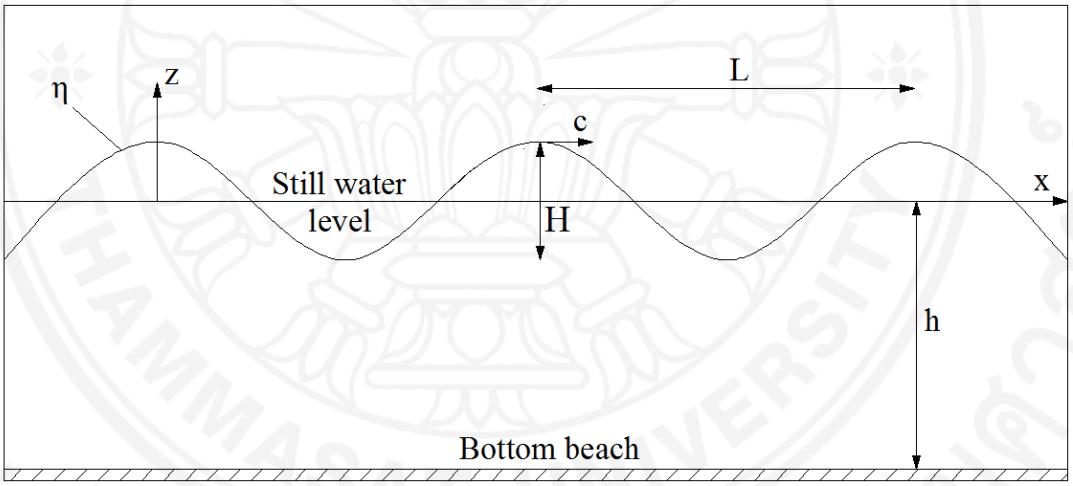

Figure 3. 1 Two-dimensional wave profile

Wave speed traveling or wave celerity is determined as:

$$c = \frac{L}{T} \tag{3.1}$$

where T is the wave period which is time required for two successive wave crest or trough to pass a specific point, L is the wave length which is the horizontal distance between two successive wave crest, and H is the vertical distance from wave crest to successive wave trough.

Other wave parameter includes:

Angular frequency: $$\sigma = \frac{2\pi}{T} \tag{3.2}$$

Wave number: $$k = \frac{2\pi}{L} \tag{3.3}$$

The variation of surface evaluation with time, from the still water level is denoted by η and given by:

$$\eta = \frac{H}{2}\cos(kx - \sigma t) \tag{3.4}$$

where x is the distance in cross shore direction, and t is the time which waves propagate.

The dispersion equation is usually used for computing k from the given h and T:

$$\sigma^2 = gk \tanh kh \tag{3.5}$$

where g is the gravity acceleration.

To simplify the calculation, k can be determined from the approximated solutions of Hunt (1979) as:

$$(kh)^2 = y^2 + \frac{y}{1 + \sum_{n=1}^{6} d_n y^n} \tag{3.6}$$

where $y = \sigma^2 h / g$, and d_n is determined form Table 3.1.

Table 3.1 Values of d_n

d_n	Values
d_1	0.6666666666
d_2	0.3555555555
d_3	0.1608465608
d_4	0.0632098765
d_5	0.021750484
d_6	0.0065407983

For particular applications, a beach profile can be classified into three regions, i.e. deep-water, intermediate depth, and shallow water regions. Limits for the three regions are shown in Table 3.2.

Table 3.2 Limits of shallow water, intermediate depth, and deep-water

Region	Limits	
	kh	*h/L*
Shallow water	$0 < kh < \frac{\pi}{10}$	$0 < \frac{h}{L} < \frac{1}{20}$
Intermediate depth	$\frac{\pi}{10} < kh < \pi$	$\frac{1}{20} < \frac{h}{L} < \frac{1}{2}$
Deep-water	$\pi < kh < \infty$	$\frac{1}{2} < \frac{h}{L} < \infty$

Using the conditions of shallow and deep-water, the equations of wave celerity, and wave length can be simplified as follows:

a) For the general condition ($0 < kh < \infty$):

$$\sigma^2 = gk \tanh kh \tag{3.7}$$

$$c = \sqrt{\frac{gL}{2\pi} \tanh kh} \tag{3.8}$$

b) For shallow water condition ($0 < kh < \pi / 10$), $\tanh kh \approx kh$:

$$c = \sqrt{gh} \tag{3.9}$$

$$L = \sqrt{ghT} \tag{3.10}$$

c) For deep-water condition ($\pi < kh < \infty$), $\tanh kh \approx 1$:

$$c_o = \frac{gT}{2\pi} \tag{3.11}$$

$$L_o = \frac{gT^2}{2\pi} \tag{3.12}$$

where c_o is deep-water wave velocity, and L_o is deep-water wave length.

3.2 Wave properties

The total energy of a progressive wave includes potential energy and kinetic energy as:

Potential energy: $$\bar{E}_p = \frac{1}{L} \int_x^{x+L} \rho g \frac{(h+\eta)^2}{2} dx \tag{3.13}$$

Kinematic energy: $$\bar{E}_k = \frac{1}{L}\int_{x}^{x+L}\int_{-h}^{\eta} \rho\frac{u^2+w^2}{2}dzdx \tag{3.14}$$

where ρ is the water density, u is the velocity in x direction, and w is the velocity in z direction.

The energy owing to the waves is different between the energy with and without waves present. Therefore, after integrating two equations above (Eqs. (3.13) and (3.14)), the potential and kinetic energy due to the waves can be expressed as:

Potential energy: $$\bar{E}_{pw} = \frac{1}{16}\rho g H^2 \tag{3.15}$$

Kinematic energy: $$\bar{E}_{kw} = \frac{1}{16}\rho g H^2 \tag{3.16}$$

The total average energy per unit surface area due to the waves is determined as follows:

$$E = \bar{E}_{pw} + \bar{E}_{kw} = \frac{1}{8}\rho g H^2 \tag{3.17}$$

When the waves propagate, the linear waves do not transfer mass. However, waves transfer the energy. The transferred energy rate is called "energy flux" which is determined as follows:

$$\bar{F}_E = \frac{1}{T}\int_{t}^{t+T}\int_{-h}^{\eta}\left(p + \frac{\rho}{2}(u^2+w^2) + \rho g z\right)udzdt \tag{3.18}$$

After altering and integrating, yield:

$$\bar{F}_E = \left(\frac{1}{8}\rho g H^2\right)\frac{\sigma}{k}\left[\frac{1}{2}\left(1+\frac{2kh}{\sinh 2kh}\right)\right] = Ecn = Ec_g \tag{3.19}$$

in which $$n = \frac{1}{2}\left(1+\frac{2kh}{\sinh 2kh}\right) \tag{3.20}$$

where c_g is the group velocity.

3.3 Wave refraction

As the wave moves over shallow water, the wave crest lines change their direction. This phenomenon causes refraction of wave. Refraction of wave occurs when the wave propagates towards shallower depth at some angles to the shoreline. Figure 3.2 shows that a wave travelling from M to N with a distance L_o and wave period T, travelling from X to Y with a smaller distance L (because c is smaller). Angle α represents the angle of wave ray to cross-shore direction, then:

$$\frac{\sin\alpha_o}{c_o} = \frac{\sin\alpha}{c} = \text{constant} \tag{3.21}$$

Equation is called "Snell's law", which is used for computing wave angle α .

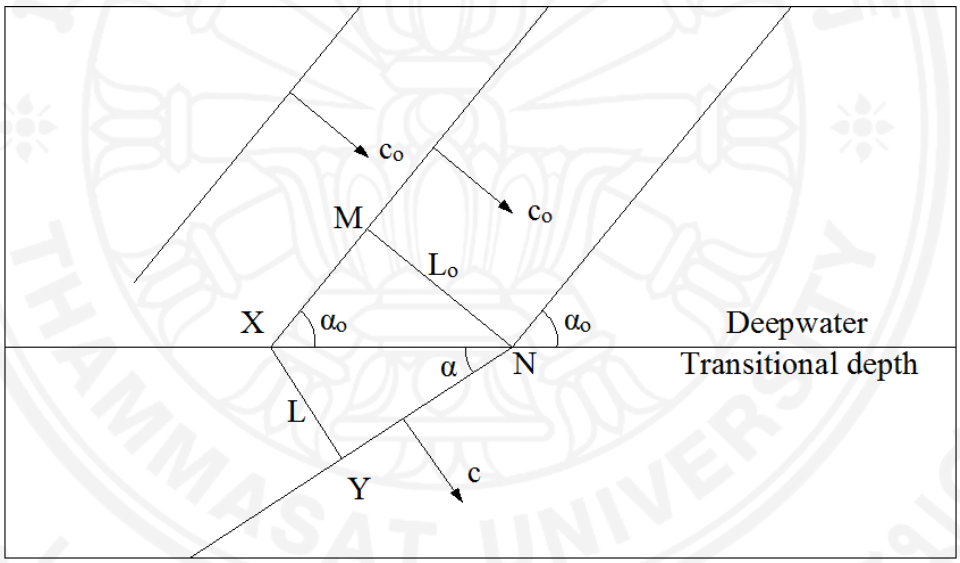

Figure 3. 2 Characteristic of wave crests during refraction

3.4 Wave transformation

As waves propagate from offshore to shoreline, wave profiles steeper and steeper. Finally waves break at breaking point and wave height decreases until all waves are broken in the inner surf zone. As the waves start to break, wave energy starts to gradually transform into turbulence and heat. The energy dissipation is conserved. The wave height transformation is computed based on the energy flux balance. The energy flux balance is described as below:

$$\frac{\partial E c_g \cos\alpha}{\partial x} = -D_B \tag{3.22}$$

where x is the distance in cross shore direction, D_B is the energy dissipation rate, and it is zero outside the surface.

Substituting Eq. (3.17) into Eq. (3.22), yield:

$$-D_B = \frac{1/8\rho g H_2^2 c_{g,2}\cos\alpha_2 - 1/8\rho g H_1^2 c_{g,1}\cos\alpha_2}{\Delta x} \tag{3.23}$$

$$\text{or } H_2 = \sqrt{\frac{1/8\rho g H_1^2 c_{g,1}\cos\alpha_1 - D_B\Delta x}{1/8\rho g c_{g,2}\cos\alpha_2}} \tag{3.24}$$

3.5 Representative wave heights

Representative wave heights are the significant parameter for both study and applications of coastal engineering field. Definition of some common representative wave heights is as follows:

a) Highest wave (H_{max}, T_{max}) is the height and the period of the highest wave in the record.

b) The highest one-tenth wave ($H_{1/10}$, $T_{1/10}$) is the average of the heights and the periods of the highest one-tenth of all waves in the record.

c) The highest one-third wave ($H_{1/3}$, $T_{1/3}$) is the average of the heights and the periods of the highest one-third of all waves in the record. $H_{1/3}$ and $T_{1/3}$ are often called significant wave height (H_s) and significant wave period (T_s).

d) Mean wave (H_m, T_m) is the average of the heights and the periods of all waves in the record.

e) Spectral root-mean-square wave (H_{rmsz}, T_{rmsz}) is defined based on the spectral approach (or energy approach) for analyzing the record data.

f) Root-mean-square wave (H_{rms}, T_{rms}) based on statistical approach (or wave-by-wave approach) is the root-mean-square of the heights and the periods of all waves in the record:

$$H_{rms} = \sqrt{\frac{\sum H_i^2}{M}} \tag{3.25}$$

$$T_{rms} = \sqrt{\frac{\sum T_i^2}{M}} \tag{3.26}$$

where M is the total number of individual waves in the record.

3.6 Measurement of model performance

The average root-mean-square relative error (ER_{avg}) is used to determine the overall accuracy of each model. The smaller value of ER_{avg}, the better accuracy of the wave model, it is defined as:

$$ER_{avg} = \frac{\sum_{n=1}^{tn} ER_{gj}}{tn} \tag{3.27}$$

where n is the data group number, ER_{gj} is the root-mean-square relative error of the group no. n, and tn is the total number of data groups.

The root-mean-square relative error of each data group (ER_g) is defined as:

$$ER_g = 100\sqrt{\frac{\sum_{i=1}^{nc}(H_{ci} - H_{mi})^2}{\sum_{i=1}^{nc} H_{mi}^2}} \tag{3.28}$$

where i is the wave height number, H_{ci} is the computed representative wave height of number i, H_{mi} is the measured representative wave height of number i, and nc is the total number of measured representative wave heights in each data group.

Rattanapitikon (2008) suggested a range of the error to determine qualitative ranking of each irregular wave model, this criterion range of each model is divided into five classes, i.e. poor ($ER_{avg} \geq 20\%$), fair ($15\% \geq ER_{avg} \geq 20\%$), good ($10\% \leq ER_{avg} \leq 15\%$), very good ($5.0\% \leq ER_{avg} \leq 10\%$), excellent ($ER_{avg} \leq 5.0\%$). The very good class and excellent class are the acceptable error ranges of each model.

3.7 Existing formulas and models

3.7.1 Breaker wave height formulas

a) In 1944 Miche proposed the criterion for maximum height of regular wave. The form is given:

$$H_b = 0.14L\tanh\left(2\pi h / \mathrm{L}\right) = 0.14L\tanh(kh) \tag{3.29}$$

where k is the positive real root of the dispersion equation.

This criterion is $H_b = 0.88h$ in shallow water. In application to random wave, the formula reduces to $H_b = \gamma h$, in which γ is an adjustable coefficient. Based on the data of experiments, Battjes and Janssen (1978) included the term $\gamma / 0.88$ in the formula of Miche (1944) and proposed that $\gamma = 0.8$. The modified formula is expressed as:

$$H_b = 0.14L \tanh\left(0.9lkh\right) \tag{3.30}$$

b) Goda (1970) based on the data of the experiments to propose a breaker wave criterion. This criterion relates to the water depth and the beach slope. The formula is as:

$$H_b = 0.17L_o \left\{1 - \exp\left[-1.5\frac{\pi h}{L_o}\left(1 + 15m_b^{4/3}\right)\right]\right\} \tag{3.31}$$

c) Thornton and Guza (1983) based on the measurement of Soldier Beach wave to suggest the similarity of breaking wave processes at two sites of the inner surf zone. The formula is as follows:

$$H_b = 0.42h \tag{3.32}$$

d) Battjes and Stive (1985) computed and compared between the computed and measured wave height in areas of breaking wave. The value of coefficient γ was given. The coefficient depends on the deep-water steepness.

$$H_b = 0.14L \tanh\left\{\left[0.57 + 0.45\tanh\left(33\frac{H_{rmso}}{L_o}\right)\right]kh\right\} \tag{3.33}$$

e) Ruessink et al. (2003) modified the breaker wave height formula by relating the coefficient to the term *kh*. Based on field-scale experiments, the formula of breaker height is proposed to be:

$$H_b = 0.14L \tanh\left[\left(0.86kh + 0.33\right)kh\right] \tag{3.34}$$

f) Apotsos et al. (2008) recalibrated the coefficient in the breaker wave height formula of eight existing dissipation models with large observation, barred and unbarred beach condition from six field-scale

experiments. The coefficient is associated with the deep-water wave height. The modified model is proposed to be:

$$H_b = 0.18 + 0.40 \tanh(0.9 H_{rmso}) h \tag{3.35}$$

3.7.2 Energy dissipation models for regular breaking wave

3.7.2.1 Bore concept

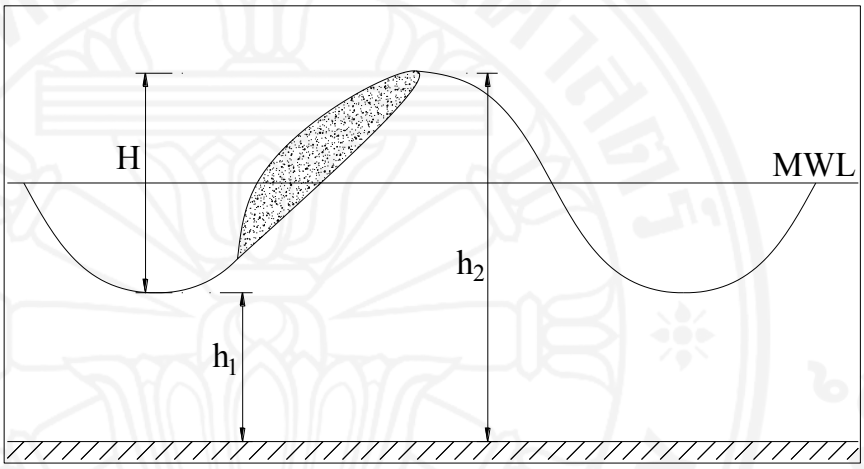

Figure 3. 3 Bore concept used to describe breaking wave

In 1962, Le Mehaute proposed that the energy dissipation caused by spilling breaker is the same as that of hydraulic jump. In the case of hydraulic jump, it is known that:

$$D_S = \frac{1}{4}\rho g \frac{(h_2 - h_1)^3}{h_1 h_2} Q = \frac{1}{4}\rho g \frac{H^3}{h_1 h_2} Q \tag{3.36}$$

where H is the breaker wave height and $H = h_2 - h_1$, ρ is the density of water, g is the gravity acceleration, h_1 and h_2 are the depth of flow before and after the hydraulic jump, and Q is the volume discharge per unit area due to the hydraulic jump. Hwang and Divoky (1970) proposed the simplest form of Q:

$$Q = \frac{ch}{L} \tag{3.37}$$

or $$Q = \frac{h}{T} \tag{3.38}$$

Substituting Eq. (3.38) into Eq. (3.36), the energy dissipation rate becomes:

$$D_S = \frac{1}{4}\frac{\rho g h H^3}{T h_1 h_2} \tag{3.39}$$

Until now, based on the bore concept, some different energy dissipation models have been proposed. Brief reviews of them can be described as follows.

a) Battjes and Janssen (1978) dropped $H/h = 1$ and assumed $h_1 h_2 = h^2$ from the order of magnitude relationship to reduce the dependence of the energy dissipation on the deep-water. The new model from the bore concept is described to be:

$$D_S = \frac{\rho g H^2}{4T} \tag{3.40}$$

b) Thornton and Guza (1983) assumed that $h_1 h_2 = h^2$ and refined the formula of Battjes and Janssen (1978). After refinement, Eq. (3.39) becomes as follows:

$$D_S = \frac{\rho g H^3}{4Th} \tag{3.41}$$

3.7.2.2 Stable energy concept

In 1985, based on the experiment data of Horikawa and Kuo (1966) on horizontal slope, Dally et al. (1985) analyzed the measured breaker wave heights and proposed this concept.

Dally et al. (1985) presumed that the energy dissipation rate is corresponding to the excess energy flux relating to the stable energy flux, divided by the water depth as:

$$D_S = \frac{K_d}{h}\left[Ec_g - (Ec_g)_{st} \right] \tag{3.42}$$

where K_d is the dimensionless decay coefficient, Ec_g is the time-averaged energy flux, $(Ec_g)_{st}$ is the energy flux associated with

the stable wave that the breaking wave is striving to attain, and subscript *st* is the variable at stable wave.

The stable wave energy density (E_{st}) and the local energy density (E) are determined as follows:

$$E_{st} = \rho g H_{st}^2 / 8 \tag{3.43}$$

$$E = \rho g H^2 / 8 \tag{3.44}$$

where H_{st} is the stable wave height.

Substituting Eq. (3.43) and Eq. (3.44) into Eq. (3.42), Eq. (3.42) becomes:

$$D_S = K_d \frac{\rho g c_g}{8h}\left[H^2 - H_{st}^2\right] \tag{3.45}$$

Dally et al. (1985) offered that the stable wave criterion is given by $H_{st} = \Gamma h$, where Γ is the dimensionless coefficient and its value appears to lie somewhere between 0.35 and 0.40.

Based on the stable energy concept, several researchers have suggested some energy dissipation models. Concise reviews of these models are shown below.

a) Dally et al. (1985) based on collected the data results of Horikawa and Kuo (1966) to propose a form of Γ. The research shown that Γ is a constant value. The optimal values of the two parameters (Γ and K_d) in the model are found to be relative constant for beaches encompassing natural slope ranges (1/80 to 1/20). The energy dissipation rate can be written as:

$$D_S = 0.15 \frac{\rho g c_g}{8h}\left[H^2 - \left(0.4h\right)_{st}^2\right] \tag{3.46}$$

b) Rattanapitikon and Shibayama (1998) determined Γ from the wave period, the water depth, and the measured wave height. The research found out that Γ and $h / \sqrt{LH}$ had the best correlation. The new form of dissipation model is shown below:

$$D_S = 0.15\frac{\rho g c_g}{8h}\left[H^2 - \left(h\exp\left(-0.36 - 1.25\frac{h}{\sqrt{LH}}\right)\right)^2\right] \quad (3.47)$$

3.7.3 Energy dissipation models for irregular breaking wave

The parametric wave models are generally based on the work of Battjes and Janssen (1978). They are modelled by using bore concept which was first proposed by Le Mehaute (1962). This approach computes only the transformation of H_{rms} in the surf zone based on the energy balance equation as:

$$\frac{\partial\left(Ec_g\cos\alpha\right)}{\partial x} = -D_B \quad (3.48)$$

in which, the wave energy density (E) can be computed as follows:

$$E = \frac{\rho g H_{rms}^2}{8} \quad (3.49)$$

In the energy flux balance equation, the wave height in the surf zone can be calculated from energy dissipation equation and parameter of previous breaker wave position with the small distance of two successive positions. However, the computation of the energy dissipation rate is a problem, it is very difficult. So far, because of the complexity of the breaking wave mechanism, the researchers proposed various energy dissipation models in the surf-zone. Concise reviews of these selected existing models are shown below.

a) Battjes and Janssen (1978) proposed the energy dissipation model by using bore concept. The model is computed by multiplying the term of energy dissipation for a single broken wave by the percentage of broken waves (Q_b). The result is as follows:

$$D_B = Q_b\frac{\rho g H_b^2}{4T_p} \quad (3.50)$$

where T_p is the spectral peak period, H_b is the breaker wave which is determined from the formula of Miche (1944), and added constant 0.91 as:

$$H_b = 0.14L\tanh(0.91kh) \tag{3.51}$$

where L is the wave length, k is the wave number, and h is the deep-water.

Polynomial equation is used for determining the fraction of broken waves as the follows:

$$Q_b = \sum_{n=0}^{7} a_n \left(\frac{H_{rms}}{H_b} \right)^n \tag{3.52}$$

where a_n is the constant of n^{th} term. The values of constants a_0 to a_7 are shown in Table 3.3.

Eq. (3.52) is used for $0.25 < H_{rms} / H_b < 0.1$. The value of Q_b can be set to zero when it is very small for $H_{rms} / H_b < 0.25$, and set to 1.0 when $H_{rms} / H_b > 0.1$.

Table 3.3 Values of a_n

a_n	Values
a_0	0.2317072
a_1	-3.6095814
a_2	22.5948312
a_3	-72.5367918
a_4	126.8704405
a_5	-120.5676384
a_6	60.7419815
a_7	-12.7250603

b) Thornton and Guza (1983) computed D_B model by integrating from 0 to ∞ the product of the energy dissipation of the single broken wave and the pdf of the breaking wave height.

$$D_B = 0.51\frac{3\sqrt{\pi}}{4}\left(\frac{H_{rms}}{H_b}\right)^4\left\{1-\frac{1}{\left[1+\left(H_{rms}/H_b\right)^2\right]^{2.5}}\right\}\frac{\rho g H_{rms}^3}{4T_p h} \quad (3.53)$$

in which the breaker height (H_b) is determined from:

$$H_b = 0.42h \quad (3.54)$$

c) Battjes and Stive (1985) changed the coefficient in the breaker height formula and used the same D_B model as that of Battjes and Janssen (1978). The coefficient relates to the deep-water wave steepness H_{rmso}/L_o, the breaker height formula is as follows:

$$H_b = 0.14L\tanh\left\{\left[0.57+0.45\tanh\left(33\frac{H_{rmso}}{L_o}\right)\right]kh\right\} \quad (3.55)$$

where H_{rmso} is the deep-water root-mean-square wave height, L_o is the deep-water wave length.

Hence, the model of Battjes and Stive (1985) is similar to that of Battjes and Janssen (1978) except the formula of H_b.

d) Southgate and Nairn (1993) proposed the same model as Battjes and Janssen (1978). The differences are the formula of energy dissipation and the formula of breaker wave height. The energy dissipation expression of breaking wave is modified from Battjes and Janssen (1978)'s the bore model to be Thornton and Guza (1983)'s the bore model as:

$$D_B = Q_b\frac{\rho g H_b^3}{4T_p h} \quad (3.56)$$

in which, Q_b is Battjes and Janssen (1978)'s the fraction of breaking waves. The breaker height formula of Nairn (1990) is completely used as:

$$H_b = h\left[0.39+0.56\tanh\left(33\frac{H_{rmso}}{L_o}\right)\right] \quad (3.57)$$

e) Baldock et al. (1998) proposed the energy dissipation model in outer and inner surf zone. The energy dissipation formula bases on Rayleigh pdf and Battjes and Janssen (1978)'s the model. H_b is from the formula of Nairn (1990):

$$D_B = \begin{cases} \exp\left[-\left(\frac{H_b}{H_{rms}}\right)^2\right]\frac{\rho g\left(H_b^2+H_{rms}^2\right)}{4T_p} & for \quad H_{rms} < H_b \\ \exp[-1]\frac{2\rho g H_b^2}{4T_p} & for \quad H_{rms} \geq H_b \end{cases} \tag{3.58}$$

$$H_b = h\left[0.39 + 0.56\tanh\left(33\frac{H_{rmso}}{L_o}\right)\right] \tag{3.59}$$

f) Rattanapitikon and Shibayama (1998) altered Battjes and Janssen (1978)'s the energy dissipation formula from the bore concept to the stable energy concept. The fraction of breaking wave and the breaking wave height are calculating based on the breaking wave criterion of Goda (1970).

$$D_B = 0.10Q_b\frac{c\rho g}{8h}\left[H_{rms}^2 - \left(h\exp(-0.58 - 2.0\frac{h}{\sqrt{LH_{rms}}})\right)^2\right] \tag{3.60}$$

$$H_b = 0.01L_o\left\{1-\exp\left[-1.5\frac{\pi h}{L_o}\left(1+15m_b^{4/3}\right)\right]\right\} \tag{3.61}$$

where m_b is the beach slope.

g) Ruessink et al. (2003) modified the coefficient of breaker wave height formula. The energy dissipation model is determined from Baldock et al. (1998). The coefficient relates to the term of kh. The modified breaker height formula is shown below:

$$H_b = 0.14L\tanh\left[\left(0.86kh + 0.33\right)kh\right] \tag{3.62}$$

h) Alsina and Baldock (2007) followed the approach of Baldock et al. (1998). However, to prevent the developed shoreline singularity in shallow water, the energy dissipation of Thornton and Guza (1983) is

replaced for Battjes and Janssen (1978)'s the bore model. The formula of breaker wave height is from the formula of Battjes and Stive (1985). They proposed the alternative dissipation model as:

$$D_B = \frac{\rho g H_{rms}^3}{4T_p h}\left\{\left[\left(\frac{H_b}{H_{rms}}\right)^3 + \frac{3}{2}\frac{H_b}{H_{rms}}\right]\exp\left[-\left(\frac{H_b}{H_{rms}}\right)^2\right] + \frac{3}{4}\sqrt{\pi}\left[1 - erf\left(\frac{H_b}{H_{rms}}\right)\right]\right\} \quad (3.63)$$

$$H_b = 0.14L\tanh\left\{\left[0.57 + 0.45\tanh\left(33\frac{H_{rmso}}{L_o}\right)\right]kh\right\} \quad (3.64)$$

i) Janssen and Battjes (2007) proposed that the energy dissipation model is determined from formula of Alsina and Baldock (2007), but the difference is the expression of breaker wave height. The breaker wave height formula is formula of Nairn (1990). The energy dissipation model and breaker wave height formula can be described as below:

$$D_B = \frac{\rho g H_{rms}^3}{4T_p h}\left\{\left[\left(\frac{H_b}{H_{rms}}\right)^3 + \frac{3}{2}\frac{H_b}{H_{rms}}\right]\exp\left[-\left(\frac{H_b}{H_{rms}}\right)^2\right] + \frac{3}{4}\sqrt{\pi}\left[1 - erf\left(\frac{H_b}{H_{rms}}\right)\right]\right\} \quad (3.65)$$

$$H_b = h\left[0.39 + 0.56\tanh\left(33\frac{H_{rmso}}{L_o}\right)\right] \quad (3.66)$$

j) Rattanapitikon and Sawanggun (2008) changed Battjes and Janssen (1978)'s the fraction expression of breaking wave model. The previous reseach based on truncated-Rayleigh dissipation to derive the formula, but Rattanapitikon and Sawanggun (2008) based on the measured wave heights to determine the fraction of breaking wave. The modified model can be written as:

$$D_B = \frac{\rho g H_b^2}{4T}\left[2.096\left(\frac{H_{rms}}{H_b}\right)^2 - 1.601\left(\frac{H_{rms}}{H_b}\right) + 0.293\right] \quad (3.67)$$

When $H_{rms}/H_b < 0.46$, D_B is set to be zero, and the breaking wave height formula of Battjes and Stive (1985) is completely used.

k) Apotsos et al. (2008) recalibrated the coefficient of the breaker wave height formula of six existing energy dissipation models. Based on two field-scale experiments, it found out that the free parameter depends on the deep-water wave height. The coefficient of the breaker height

formula is modified until the smallest error is obtained. The modified model is written as follows:

$$D_B = \frac{3\sqrt{\pi}}{4}\left(\frac{H_{rms}}{H_b}\right)^2 \left\{1 - \frac{1}{\left[1+\left(H_{rms}/H_b\right)^2\right]^{2.5}}\right\} \frac{\rho g H_{rms}^3}{4T_p h} \tag{3.68}$$

in which the value of H_b is determined from:

$$H_b = \left[0.18 + 0.4\tanh\left(0.9H_{rmso}\right)\right]h \tag{3.69}$$

Chapter 4
Collected Experimental Data

Experimental data of representative wave heights transformation across-shore from 14 sources (including 1732 cases) are compiled for examining and developing the models of irregular wave. Total number of compiled data points for H_m, H_{rms}, $H_{1/3}$, $H_{1/10}$, and H_{rmsz} are 2299, 5783, 5878, 5627, and 17848, respectively. A summary of the compiled data points is shown in Table 4.1.

The compiled data include a wide range of beach conditions, i.e. sand beach (SB), stepped beach (STB), barred beach (PB), and plane beach (PB). Based on the experiment scale, the data are divided into 3 experimental groups, i.e. field-scale (FS), large-scale (LS), and small-scale (SS) experiments. The experiments of Smith and Kraus (1990), Hurue (1990), Katayama (1991), Smith and Vincent (1992), Smith and Seabergh (2001), Hamilton and Ebersole (2001), and Ting (2001) are processed under fixed bed conditions with small-scale wave channel, the experiments of Kraus and Smith (1994), Roelvink and Reniers (1995), and Dette et al. (1998) are performed in large-scale, the experiments of Hotta et al. (1982), Thornton and Guza (1986), Birkemeier et al. (1997), and Herbers et al. (2006) are performed in field-scale with movable bed conditions. Concise reviews of some experiments are shown as below:

Table 4. 1 Summary of collected experimental data

Sources	No. of cases	No. of data					Beach conditions	Apparatus
		H_m	H_{rms}	$H_{1/3}$	$H_{1/10}$	H_{rmsz}		
Smith and Kraus (1990)	12	96	96	96	-	-	PB and BB	SS
Hurue (1990)	1	-	-	7	-	-	PB	SS
Katayama (1991)	2	-	-	16	-	-	BB	SS
Smith and Vincent (1992)	4					36	PB	SS
Smith and Seabergh (2001)	11	132	-	132	-	132	STB	SS
Hamilton and Ebersole (2001)	1					10	PB	SS
Ting (2001)	1	7	7	7	7	-	PB	SS
Kraus and Smith (1994)	128	2046	2046	2046	2046	2046	SB	LS
Roelvink and Reniers (1995)	95	-	-	-	-	923	SB	LS
Dette et al. (1998)	138	-	3556	3556	3556	3556	SB	LS
Hotta et al. (1982)	3	18	18	18	18		SB	FS
Thornton and Guza (1986)	4	-	60	-	-	-	SB	FS
Birkemeier et al.(1997)	745	-	-	-	-	5043	SB	FS
Herbers et al. (2006)	587	-	-	-	-	6102	SB	FS
Total	1732	2299	5783	5878	5627	17848		

Remarks: PB = plane beach BB = barred beach STB = stepped beach SB = sand beach
FS = field-scale LS = large-scale SS = small-scale

a) The experiment of Kraus and Smith (1994) (The SUPERTANK laboratory data collection project) was carried out to compile data to develop numerical simulation model of study cross-shore sand transportation, hydrodynamic and beach profile. The project was processed from August 5 to September 13, 1991. A large wave tank was 4.6 m deep, 104 m long, and 3.7 m wide and SUPERTANK project constructed a sandy beach of 76 m long. This project was applied for irregular and regular wave. The experiments of irregular wave comprised 128 cases with moveable bed conditions. Wave was generated with spectral width parameter between 3.3 and 100, spectral peak periods from 3.0 s to 10.0 s, and the zero moment wave heights from 0.2 m to 1.0 m. In across shore direction, the channel used sixteen resistance wave gages. All data processing the wave spectral analysis were used in this study.

b) The experiment of Dette et al. (1998) (SAFE Project) was carried out to develop protection and design of coastal structures of beach nourishment. The data would contribute to calibrate and validate the modelling tools. The SAFE Project included four topics and a large-scale experiment. A large wave tank was 7 m deep, 5 m wide, and 300 m long, a sandy beach which was constructed into was 250 m long. The project was consisted of two main sections. The first section was to research equilibrium profile under changed beach slope condition. The second section was aimed to investigate experiment on beach and dune stability. The tests were processed for both with and without storm wave conditions. The channel was instrumented with twenty-seven resistance wave gages. The compiled experiments comprised 138 cases.

c) The experiment of Smith and Kraus (1990) was carried out to study the macro-features of breaking wave over a range of bar and reef geometries, wave periods, and wave heights for a fixed water level. The tank which was 0.91 m deep, 0.46 m wide, and 45.7 m long was constructed. This project comprised regular and irregular wave. The irregular wave tests consisted of 12 cases. Both bar beach and plane beach generated three irregular wave conditions. Wave was run with spectral peak periods 1.07 s, 1.56 s, and 1.75 s, spectral width parameter 3.3, and the zero moment wave heights 0.12 m, 0.15 m, and 0.14 m. A total of eight wave gages were used for measuring water surface elevations.

d) The experiment of Ting (2001) was carried out on a broad-banded irregular wave to investigate the characteristics of turbulence velocities and wave in the surf

zone. The tests were processed in 1.22 m deep, 0.91 m wide and 37 m long glass-walled tank. The plane bottom by marine plywood was designed with 1/35 uniform slope. Wave conditions for the study were peak spectral period 2.0 s. All waves were generated with the TMA spectrum Bouws et al. (1985) by using a gamma value 3.30 and zero moment wave height 0.15 m. The duration of the collection data from the start of generation was 8.192 min. The tank was instrumented with seven resistance-type gages.

e) The experiment of Smith and Seabergh (2001) was made in the 3D (three-dimensional) Idealized Inlet Laboratory with a steady ebb current to examine wave breaking on a current through physical-model measurements. This study was applied for regular and irregular wave. The large tank which was constructed for the experiment was 99 m long, 46 m wide, and 0.6 m deep. All waves were run with the Texel, Marsen, and Arsloe (TMA) spectral form (Bouws et al. (1985)) by using a gamma value 3.30 and zero moment wave heights 3.7 cm and 5.5 cm, and peak spectral periods 0.7 s and 1.4 s. A total of eleven wave gages were used for measuring water surface elevations.

f) The experiment of Smith and Vincent (1992) was carried out to examine the multiple irregular wave trains shoaling and decay. Waves were run with the TMA spectral form (Bouws et al. (1985)) using a gamma value 20, zero-moment wave heights 0.15 m and 0.9 m, double-peaked spectra 2.5 s/ 1.25s and 2.5 s/ 1.75 s. This experiment used a flume of 0.45 m wide, 0.9 m deep, and 45.7 m long. The plane bottom with 1/30 uniform slope was designed by concrete from the middle of the channel. A total of nine electrical resistance gages were used for measuring water surface elevations.

g) The experiment of Hamilton and Ebersole (2001) was carried out to study uniform long-shore currents in a wave basin. The small-scale wave tank of 50 m long, 30 m wide, and 1.4 m deep was constructed. The beach of 21 m wide and 31 m long with 1/30 uniform slope was designed by concrete. Waves were run with the TMA spectral form (Bouws et al. (1985)) using a gamma value 3.3, zero moment wave height 0.21 m, direction 10^{o}, and spectral peak period 2.5 s. In cross-shore direction, ten electrical resistance gages were used for measuring water surface elevations and near the wave generators in the long-shore direction four wave gages were installed.

h) The experiment of Roelvink and Reniers (1995) (LIP 11D Delta Flume Experiment) was instigated at Delft Hydraulics' Delta Flume. The project constructed

a sandy beach of 175 m long in a tank of 5 m wide, 7 m deep, and 233 m long. The experiment included dune and no dune. Each experiment was processed under wave conditions, and about 12–21 hr for each condition. Initial geometry of tests no. 1A and 2A were equilibrium Dean-type beaches with constant slope near and above the water line, and the initial geometry of test no. 1B, 1C, 2B, 2E, and 2C were final geometry of the preceding test. Total of 94 cases of wave were performed under beach conditions. All waves were generated with JONSWAP spectrum (Hasselmann et al. (1973)) by using a gamma value 3.3, zero moment wave heights from 0.6 m to 1.4 m, water level from 4.1 m to 4.6 m, and spectral peak periods from 5 s to 8 s. A total of ten resistance gages were used for measuring water surface elevations.

i) The experiment of Birkemeier et al. (1997) (DELILAH Project) was carried out to study the barred beach to develop basic understanding and surf zone physical model in October 1990. The Experiment occurred in Duck, North Carolina, USA. Nine pressure gauges were used for measuring water surface elevations. Water surface elevations determined the significant wave heights based on the frequency band 0.04–0.4 Hz. The experiment covered wave periods from 3.4 s to 13.5 s and zero moment wave heights from 0.4 m to 0.7 m. The 776 data of the wave heights and the water depths were obtained at roughly every 34 min. However, some points of measurements were not suitable for applying to the irregular wave models, the study considered 745 data.

j) The experiment of Herbers et al. (2006) (DUCK94 Project) was carried out to study the barred beach during Aug–Oct 1994. The experiment occurred in Duck, North Carolina, USA and had the same objective as DELILAH. The experiment added components to resolve sediment transport and morphologic evolution at bed form scales from ripples to near-shore bars. Thirteen pressure gauges were used for measuring water surface elevations. Water surface elevations determined the significant wave heights based on the frequency band 0.05–0.25 Hz. The present study used the obtained value of wave heights and water depths at every 3 h. The study considered 587 data. The experiment covered wave periods from 4.4 s to 11.4 s and zero moment wave heights from 0.2 m to 2.6 m.

k) The experiment of Katayama (1991) was carried out to research wave and undertow velocity on a bar-type beach. A wave tank with small-scale of 17 m long, 0.5

m wide, and 0.55 m deep was constructed. The bar-type beach included three types of slope, the first 5 m of 1/20, the next 1 m of -1/20, and the last 4 m of 1/20 slope. Irregular wave was run with the Bretschneider Mitsuyasu spectrum (Bretschneider (1968), Mitsuyasu (1970)) by using wave periods 0.95 s and 1.14 s and the zero moment wave heights 0.06 m and 0.08 m. Total of eight resistance gages were used for measuring water surface elevations

l) The experiment of Hurue (1990) was carried out to investigate undertow velocity and wave on a plane beach. A wave tank with small-scale was 17 m long, 0.5 m wide, and 0.55 m deep. The smooth bottom with 1/20 uniform slope was designed. The experiment was performed for regular and irregular wave. Irregular wave was run with the Bretschneider Mitsuyasu spectrum (Bretschneider (1968), Mitsuyasu (1970)) by using wave period 1.26 s and zero moment wave height 0.09 m. A total of seven resistance gages were used for measuring water surface elevations

m)The experiment of Hotta et al. (1982) was carried out to extensive field studies to better understand the characteristics of waves in the near-shore zone at Ajigaura beach facing the Pacific Ocean, and located about 200 km north of Tokyo. Direct application of the zero-crossing methods created a problem for defining waves in the near-shore zone. In this study, the data given by the zero-up crossing method were used. A total of seven resistance gages were used for measuring water surface elevations. Excluding a few data was not suitable for applying to the irregular wave models, a total of 18 cases of wave were performed under beach conditions.

Chapter 5
Existing Model Examination

5.1 Parametric wave approach

The parametric wave models are considered in this study. As the previous section mentioned that the transformation of H_{rms} would be predicted by using the energy flux conservation law and the expression can be described as:

$$\frac{\rho g}{8}\frac{\partial\left(Ec_g\right)}{\partial x} = -D_B \tag{5.1}$$

where the wave energy density (E) can be computed as follows:

$$E = \frac{\rho g H_{rms}^2}{8} \tag{5.2}$$

Substituting Eq. (5.2) into Eq. (5.1), yield:

$$-D_B = \frac{1/8\,\rho g H_{rms2}^2 c_{g,2}\cos\alpha_2 - 1/8\,\rho g H_{rms1}^2 c_{g,1}\cos\alpha_2}{\Delta x} \tag{5.3}$$

$$\text{or } H_{rms2} = \sqrt{\frac{1/8\,\rho g H_{rms1}^2 c_{g,1}\cos\alpha_1 - D_B\Delta x}{1/8\,\rho g c_{g,2}\cos\alpha_2}} \tag{5.4}$$

In the present section, Eq. (5.1) is applied directly to compute root-mean-square wave height. The selected D_B models (based on the parametric wave approach) are shown in Table 5.1 together with their abbreviations. It can be seen from Table 5.1 that the energy dissipation rate (D_B) has the relationship with various variables, i.e. deep-water wave length (L_o), deep-water root-mean-square wave height (H_{rmso}), root-mean-square wave height (H_{rms}), water depth (h), spectral peak period (T_p), fraction of wave breaking (Q_b), breaker height (H_b), phase velocity (c), bottom slope (m_o), wave length (L), and wave number (k).

Table 5.1 The existing wave energy dissipation models

Sources	Models
Battjes and Janssen (1978): BJ78	$D_B = Q_b \frac{\rho g H_b^2}{4T_p}$ $\frac{1-Q_b}{-\ln Q_b} = \left(\frac{H_{rms}}{H_b}\right)^2$ $H_b = K_1 L \tanh\left(0.91kh\right)$
Thornton and Guza (1983): TG83	$D_B = 0.51 \frac{3\sqrt{\pi}}{4} \left(\frac{H_{rms}}{H_b}\right)^2 \left\{1 - \frac{1}{\left[1+\left(H_{rms}/H_b\right)^2\right]^{2.5}}\right\} \frac{\rho g H_{rms}^3}{4T_p h}$ $H_b = K_2 h$
Battjes and Stive (1985): BS85	$D_B = Q_b \frac{\rho g H_b^2}{4T_p}$ $\frac{1-Q_b}{-\ln Q_b} = \left(\frac{H_{rms}}{H_b}\right)^2$ $H_b = K_3 L \tanh\left\{\left[0.57 + 0.45 \tanh\left(33 \frac{H_{rmso}}{L_o}\right)\right] kh\right\}$
Southgate and Nairn (1993): SN93	$D_B = Q_b \frac{\rho g H_b^3}{4T_p h}$ $\frac{1-Q_b}{-\ln Q_b} = \left(\frac{H_{rms}}{H_b}\right)^2$ $H_b = K_4 h \left[0.39 + 0.56 \tanh\left(33 \frac{H_{rmso}}{L_o}\right)\right]$

Table 5.1(cont.) The existing wave energy dissipation models

Sources	Models
Baldock et al. (1998): BHV98	$D_B = \begin{cases} exp\left[-\left(\frac{H_b}{H_{rms}}\right)^2\right]\frac{\rho g\left(H_b^2+H_{rms}^2\right)}{4T_p} & for \quad H_{rms} < H_b \\ exp[-1]\frac{2\rho g H_b^2}{4T_p} & for \quad H_{rms} \geq H_b \end{cases}$ $H_b = K_5 h\left[0.39 + 0.56\tanh\left(33\frac{H_{rmso}}{L_o}\right)\right]$
Rattanapitikon and Shibayama (1998): RS98	$D_B = 0.10 Q_b \frac{c\rho g}{8h}\left[H_{rms}^2 - \left(h\exp(-0.58 - 2.0\frac{h}{\sqrt{LH_{rms}}})\right)^2\right]$ $\frac{1-Q_b}{-\ln Q_b} = \left(\frac{H_{rms}}{H_b}\right)^2$ $H_b = K_6 L_o\left\{1 - \exp\left[-1.5\frac{\pi h}{L_o}\left(1+15m_b^{4/3}\right)\right]\right\}$
Ruessink et al. (2003): RWS03	$D_B = \begin{cases} \exp\left[-\left(\frac{H_b}{H_{rms}}\right)^2\right]\frac{\rho g\left(H_b^2+H_{rms}^2\right)}{4T_p} & for \quad H_{rms} < H_b \\ \exp[-1]\frac{2\rho g H_b^2}{4T_p} & for \quad H_{rms} \geq H_b \end{cases}$ $H_b = K_7 L\tanh\left[(0.86kh + 0.33)kh\right]$
Alsina and Baldock (2007): AB07	$D_B = \frac{\rho g H_{rms}^3}{4T_p h}\left\{\left[\left(\frac{H_b}{H_{rms}}\right)^3 + \frac{3}{2}\frac{H_b}{H_{rms}}\right]\exp\left[-\left(\frac{H_b}{H_{rms}}\right)^2\right] + \frac{3}{4}\sqrt{\pi}\left[1 - erf\left(\frac{H_b}{H_{rms}}\right)\right]\right\}$ $H_b = K_8 L\tanh\left\{\left[0.57 + 0.45\tanh\left(33\frac{H_{rmso}}{L_o}\right)\right]kh\right\}$

Table 5.1(cont.) The existing wave energy dissipation models

Sources	Models
Janssen and Battjes (2007): JB07	$D_B = \frac{\rho g H_{rms}^3}{4T_p h}\left\{\left[\left(\frac{H_b}{H_{rms}}\right)^3 + \frac{3}{2}\frac{H_b}{H_{rms}}\right]\exp\left[-\left(\frac{H_b}{H_{rms}}\right)^2\right] + \frac{3}{4}\sqrt{\pi}\left[1 - erf\left(\frac{H_b}{H_{rms}}\right)\right]\right\}$ $H_b = K_9 h\left[0.39 + 0.56\tanh\left(33\frac{H_{rmso}}{L_o}\right)\right]$
Rattanapitikon and Sawanggun (2008): RS08	$D_B = \frac{\rho g H_b^2}{4T}\left[2.096\left(\frac{H_{rms}}{H_b}\right)^2 - 1.601\left(\frac{H_{rms}}{H_b}\right) + 0.293\right]$ $H_b = K_{10} L\tanh\left\{\left[0.57 + 0.45\tanh\left(33\frac{H_{rmso}}{L_o}\right)\right]kh\right\}$
Apotsos et al. (2008): AREG08	$D_B = \frac{3\sqrt{\pi}}{4}\left(\frac{H_{rms}}{H_b}\right)^2\left\{1 - \frac{1}{\left[1 + \left(H_{rms}/H_b\right)^2\right]^{2.5}}\right\}\frac{\rho g H_{rms}^3}{4T_p h}$ $H_b = K_{11}[0.18 + 0.40\tanh(0.9H_{rmso})]h$

5.2 Model examination with default coefficient

The transformation of representative wave heights is determined by substituting each dissipation model (shown in Table 5.1) into Eq. (5.4) to solve the differential equations. The input data are the beach profile (h and x), the coefficient, the spectral peak period, and the incident wave height. The computation is processed from offshore to shoreline by using the collected data shown in Table 4.1. The compiled data are divided into 3 groups, i.e. field-scale, large-scale, and small-scale experiments. The errors of the models are determined from Eqs. (3.27) and (3.28). By using the default coefficients, the errors of the existing models on simulating H_{rms} are shown in Table 5.2.

Table 5.2 The average error of each model for predicting transformation of H_{rms} by using the default coefficients

Resources	Default coefficients	SS	LS	FS	ER_{avg}
BJ78	$K_1 = 0.14$	9.3	6.6	18.9	11.6
TG83b	$K_2 = 0.42$	28.0	10.4	14.0	17.4
BS85	$K_3 = 0.14$	8.6	9.8	14.5	11.0
SN93	$K_4 = 1.0$	13.1	7.6	20.8	13.8
BHV98	$K_5 = 1.0$	12.5	10.8	17.7	13.6
RS98	$K_6 = 0.17$	11.7	7.9	13.4	11.0
RWS03	$K_7 = 0.14$	14.1	10.8	16.6	13.8
AB07	$K_8 = 0.14$	7.6	8.1	14.7	10.1
JB07	$K_9 = 1.0$	9.7	8.9	14.7	11.1
RS08	$K_{10} = 0.14$	8.5	9.5	13.6	10.5
AREG08	$K_{11} = 1.0$	30.9	9.9	14.1	18.3

Remarks: FS = field-scale LS = large-scale SS = small-scale

The model of AB07 gives the best prediction in estimating H_{rms} (ER_{avg} = 10.1%), however, this average error is still large (>10%). Hence, by recalibrating the model, the result of each model should be better and more suitable for computing transformation of H_{rms} than that of existing models.

Chapter 6

Model Development for Computing Root-Mean-Square Wave Height

6.1 New energy dissipation formulation

The aim of this section is to develop a new model by applying the energy dissipation formulation of Dally et.al (1985) to Baldock et al. (1998)'s the D_B model.

Firstly, multiplying the energy dissipation formulation (D_S) of Dally et al. (1985) by the pdf of the breaking wave heights. Then integrating that product from H_b to ∞ to compute the total energy dissipation:

$$D_B = \int_{H^*}^{\infty} D_S p\left(\frac{H}{H_{rms}}\right) d\left(\frac{H}{H_{rms}}\right) \tag{6.1}$$

The distribution pdf of Rayleigh is as below:

$$p\left(\frac{H}{H_{rms}}\right) = 2\frac{H}{H_{rms}} \exp\left[-\left(\frac{H}{H_{rms}}\right)^2\right] \tag{6.2}$$

Dally et al. (1985) suggested the energy dissipation formulation as follows

$$\langle D_S \rangle = 0.15\frac{\rho g c_g}{8h}\left(H^2 - H_{st}^2\right) = 0.15\frac{c_g}{h}\left(E - E_{st}\right) \tag{6.3}$$

Substitute Eq. (6.3) into Eq. (6.1), yield:

$$D_B = \int_{H^*}^{\infty} 0.15\frac{\rho g c_g}{8h}\left[H^2 - H_{st}^2\right] p\left(\frac{H}{H_{rms}}\right) d\left(\frac{H}{H_{rms}}\right) \tag{6.4}$$

where $H^* = H_b / H_{rms}$.

Analytical integration of Eq. (6.4), gives:

$$D_B = exp\left[-\left(\frac{H_b}{H_{rms}}\right)^2\right] \frac{0.15\rho g c_g\left[H_b^2 + H_{rms}^2 - H_{st}^2\right]}{8h} \tag{6.5}$$

where H_{st} is the stable wave height.

Dally et al. (1985) suggested that H_{st} can be computed as follows:

$$H_{st} = \Gamma h \tag{6.6}$$

where $\Gamma = 0.4$ is the stable wave factor.

This study collects seven existing breaker wave height (H_b) formulas, which were used in the parametric wave approach for developing the new model, i.e. Miche (1944), Goda (1970), Thornton and Guza (1983), Battjes and Stive (1985), Southgate and Nairn (1990), Ruessink et al. (2003), and Apotsos et al. (2008). Each breaker wave height formula would be substituted into the present energy dissipation formula for computing energy dissipation wave. The new models are shown in Table 6.1.

Table 6.1 The present models for predicting transformation of H_{rms}

Sources	Models
MD1	$\mathrm{D}_B = 0.15\rho g c_g \exp\left[-\left(\frac{H_b}{H_{rms}}\right)^2\right]\frac{\left[H_b^2 + H_{rms}^2 - (0.4h)^2\right]}{8h}$ $H_b = K_{12} L \tanh(0.91kh)$
MD2	$\mathrm{D}_B = 0.15\rho g c_g \exp\left[-\left(\frac{H_b}{H_{rms}}\right)^2\right]\frac{\left[H_b^2 + H_{rms}^2 - (0.4h)^2\right]}{8h}$ $H_b = K_{13} L_o \left\{1 - \exp\left[-1.5\frac{\pi h}{L_o}\left(1 + 15 m_b^{4/3}\right)\right]\right\}$
MD3	$\mathrm{D}_B = 0.15\rho g c_g \exp\left[-\left(\frac{H_b}{H_{rms}}\right)^2\right]\frac{\left[H_b^2 + H_{rms}^2 - (0.4h)^2\right]}{8h}$ $H_b = K_{14} h$
MD4	$\mathrm{D}_B = 0.15\rho g c_g \exp\left[-\left(\frac{H_b}{H_{rms}}\right)^2\right]\frac{\left[H_b^2 + H_{rms}^2 - (0.4h)^2\right]}{8h}$ $H_b = K_{15} L \tanh\left\{\left[0.57 + 0.45\tanh\left(33\frac{H_{rmso}}{L_o}\right)\right]kh\right\}$

Table 6.1(cont.) The developed model for predicting transformation of H_{rms}

Sources	Models
MD5	$\mathrm{D}_B = 0.15\rho g c_g \exp\left[-\left(\frac{H_b}{H_{rms}}\right)^2\right]\frac{\left[H_b^2 + H_{rms}^2 - (0.4h)^2\right]}{8h}$ $H_b = K_{16}h\left[0.39 + 0.56\tanh\left(33\frac{H_{rmso}}{L_o}\right)\right]$
MD6	$\mathrm{D}_B = 0.15\rho g c_g \exp\left[-\left(\frac{H_b}{H_{rms}}\right)^2\right]\frac{\left[H_b^2 + H_{rms}^2 - (0.4h)^2\right]}{8h}$ $H_b = K_{17}L\tanh\left[(0.86kh + 0.33)kh\right]$
MD7	$\mathrm{D}_B = 0.15\rho g c_g \exp\left[-\left(\frac{H_b}{H_{rms}}\right)^2\right]\frac{\left[H_b^2 + H_{rms}^2 - (0.4h)^2\right]}{8h}$ $H_b = K_{18}[0.18 + 0.40\tanh(0.9H_{rms})]h$

where K_{12}, K_{13}, K_{14}, K_{15}, K_{16}, K_{17}, and K_{18} are the coefficients. The default coefficients are shown in Table 6.2.

Table 6.2 The default coefficients of the breaker height formulas

Coefficient	Value
K_{12}	0.14
K_{13}	0.17
K_{14}	0.42
K_{15}	0.14
K_{16}	1.00
K_{17}	0.14
K_{18}	1.0

6.2 Model examination

To examine the models shown in Table 6.1 and to determine the best model for calculating transformation of H_{rms}, this section would compute the overall accuracy of each model. The best model is the model which gives the best accuracy (the smallest error).

The transformation of H_{rms} is determined by substituting each dissipation model (shown in Table 6.1) into Eq. (5.4) to resolve the differential equations. The input data are the beach profile (h and x), the incident wave height, the spectral peak period, and other calibrated variables. The computation is processed from offshore to shoreline by using the collected data shown in Table 4.1. The data are divided 3 groups, i.e. field-scale, large-scale, and small-scale experiments. The errors of the models are determined from Eqs. (3.27) and (3.28). By using the default coefficients, the errors of the collected models on simulating H_{rms} are shown in Table 6.3.

Table 6.3 The average error of present models for predicting transformation of H_{rms} by using the default coefficients

Resources	Default coefficients	SS	LS	FS	ER_{avg}
MD1	$K_{12} = 0.14$	9.0	6.2	10.5	8.6
MD2	$K_{13} = 0.17$	11.4	6.5	15.5	11.1
MD3	$K_{14} = 0.42$	14.0	14.7	16.1	14.9
MD4	$K_{15} = 0.14$	9.2	8.5	11.5	9.7
MD5	$K_{16} = 1.0$	13.4	9.5	13.9	12.2
MD6	$K_{17} = 0.14$	11.5	9.8	12.8	11.3
MD7	$K_{18} = 1.0$	10.1	9.9	11.2	10.4

Remarks: FS = field-scale LS = large-scale SS = small-scale

The MD1 model gives the best prediction in estimating H_{rms} (ER_{avg}=8.6%). But the coefficients of each collected model may not be the best values to compute H_{rms}

.Hence, the coefficients of all models should be recalibrated before applying to the models, and the errors of each model should be improved.

Chapter 7
Model Extension

7.1 Models consideration

Parametric wave approach only computes transformation of H_{rms}. However, the previous experiments shown that the representative wave heights transform in the same fashion. This section would apply to 12 models (11 existing models and a present model) shown in Table 7.1, for calculating representative wave heights (i.e. H_m, $H_{1/3}$, $H_{1/10}$, H_{rms}, and H_{rmsz}) transformation.

Pre-calibrations were performed to investigate the effect of coefficients (in the selected models) on the accuracy of the models. The pre-calibrations revealed that only one coefficient has significant effect on the transformation of various representative wave heights. Therefore, only a coefficient (K) in each D_B model (shown in Table 7.1) is introduced to consider its effect on the transformation of different representative wave heights.

Table 7.1 The collected wave energy dissipation models for calibration

Sources	Models
Battjes and Janssen (1978): BJ78	$D_B = Q_b \frac{\rho g H_b^2}{4T_p}$ $\quad \frac{1-Q_b}{-\ln Q_b} = \left(\frac{H_{rms}}{H_b}\right)^2$ $H_b = K_1 L \tanh(0.91kh)$
Thornton and Guza (1983): TG83	$D_B = 0.51 \frac{3\sqrt{\pi}}{4} \left(\frac{H_{rms}}{H_b}\right)^2 \left\{1 - \frac{1}{\left[1+\left(H_{rms}/H_b\right)^2\right]^{2.5}}\right\} \frac{\rho g H_{rms}^3}{4T_p h}$ $H_b = K_2 h$
Battjes and Stive (1985): BS85	$D_B = Q_b \frac{\rho g H_b^2}{4T_p}$ $\quad \frac{1-Q_b}{-ln Q_b} = \left(\frac{H_{rms}}{H_b}\right)^2$ $H_b = K_3 L \tanh\left\{\left[0.57 + 0.45 \tanh\left(33 \frac{H_{rmso}}{L_o}\right)\right] kh\right\}$

Table 7.1(cont.) The collected wave energy dissipation models for calibration

Sources	Models
Southgate and Nairn (1993): SN93	$D_B = Q_b \frac{\rho g H_b^3}{4T_p h}$ $\quad \frac{1-Q_b}{-\ln Q_b} = \left(\frac{H_{rms}}{H_b}\right)^2$ $H_b = K_4 h\left[0.39 + 0.56\tanh\left(33\frac{H_{rmso}}{L_o}\right)\right]$
Baldock et al. (1998): BHV98	$D_B = \begin{cases} exp\left[-\left(\frac{H_b}{H_{rms}}\right)^2\right]\frac{\rho g\left(H_b^2+H_{rms}^2\right)}{4T_p} & for \quad H_{rms} < H_b \\ exp[-1]\frac{2\rho g H_b^2}{4T_p} & for \quad H_{rms} \geq H_b \end{cases}$ $H_b = K_5 h\left[0.39 + 0.56\tanh\left(33\frac{H_{rmso}}{L_o}\right)\right]$
Rattanapitikon and Shibayama (1998): RS98	$D_B = 0.10 Q_b \frac{c\rho g}{8h}\left[H_{rms}^2 - \left(h\exp(-0.58 - 2.0\frac{h}{\sqrt{LH_{rms}}})\right)^2\right]$ $\frac{1-Q_b}{-\ln Q_b} = \left(\frac{H_{rms}}{H_b}\right)^2$ $H_b = K_6 L_o\left\{1 - \exp\left[-1.5\frac{\pi h}{L_o}\left(1 + 15 m_b^{4/3}\right)\right]\right\}$
Ruessink et al. (2003): RWS03	$D_B = \begin{cases} \exp\left[-\left(\frac{H_b}{H_{rms}}\right)^2\right]\frac{\rho g\left(H_b^2+H_{rms}^2\right)}{4T_p} & for \quad H_{rms} < H_b \\ \exp[-1]\frac{2\rho g H_b^2}{4T_p} & for \quad H_{rms} \geq H_b \end{cases}$ $H_b = K_7 L\tanh\left[\left(0.86kh + 0.33\right)kh\right]$

Table 7.1(cont.) The collected wave energy dissipation models for calibration

Sources	Models
Alsina and Baldock (2007): AB07	$D_B = \frac{\rho g H_{rms}^3}{4T_p h}\left\{\left[\left(\frac{H_b}{H_{rms}}\right)^3 + \frac{3}{2}\frac{H_b}{H_{rms}}\right]\exp\left[-\left(\frac{H_b}{H_{rms}}\right)^2\right] + \frac{3}{4}\sqrt{\pi}\left[1 - erf\left(\frac{H_b}{H_{rms}}\right)\right]\right\}$ $H_b = K_8 L \tanh\left\{\left[0.57 + 0.45\tanh\left(33\frac{H_{rmso}}{L_o}\right)\right]kh\right\}$
Janssen and Battjes (2007): JB07	$D_B = \frac{\rho g H_{rms}^3}{4T_p h}\left\{\left[\left(\frac{H_b}{H_{rms}}\right)^3 + \frac{3}{2}\frac{H_b}{H_{rms}}\right]\exp\left[-\left(\frac{H_b}{H_{rms}}\right)^2\right] + \frac{3}{4}\sqrt{\pi}\left[1 - erf\left(\frac{H_b}{H_{rms}}\right)\right]\right\}$ $H_b = K_9 h\left[0.39 + 0.56\tanh\left(33\frac{H_{rmso}}{L_o}\right)\right]$
Rattanapitikon and Sawanggun (2008): RS08	$D_B = \frac{\rho g H_b^2}{4T}\left[2.096\left(\frac{H_{rms}}{H_b}\right)^2 - 1.601\left(\frac{H_{rms}}{H_b}\right) + 0.293\right]$ $H_b = K_{10} L \tanh\left\{\left[0.57 + 0.45\tanh\left(33\frac{H_{rmso}}{L_o}\right)\right]kh\right\}$
Apotsos et al. (2008): AREG08	$D_B = \frac{3\sqrt{\pi}}{4}\left(\frac{H_{rms}}{H_b}\right)^2\left\{1 - \frac{1}{\left[1 + \left(H_{rms}/H_b\right)^2\right]^{2.5}}\right\}\frac{\rho g H_{rms}^3}{4T_p h}$ $H_b = K_{11}[0.18 + 0.40\tanh(0.9H_{rmso})]h$
MD1	$\mathrm{D}_B = 0.15\rho g c_g \exp\left[-\left(\frac{H_b}{H_{rms}}\right)^2\right]\frac{\left[H_b^2 + H_{rms}^2 - \left(0.4h\right)^2\right]}{8h}$ $H_b = K_{12} L \tanh\left(0.9lkh\right)$

7.2 Model calibration for computing representative wave heights

The transformation of each representative wave height is determined by substituting each dissipation model (shown in Table 7.1) into Eq. (5.4) and replacing H_{rms} by each representative wave height (H_m, H_{rmsz}, $H_{1/3}$, and $H_{1/10}$) to resolve the differential equations. After that, the input data are the beach profile (h and x), the incident wave height, the spectral peak period, and other calibrated variables. The computation is processed form offshore to shoreline by using the collected data shown in Table 4.1. The compiled data are divided into 3 groups, i.e. field-scale, large-scale and small-scale experiments. The errors of the models are determined from Eqs. (3.27) and (3.28).

This section would calibrate the coefficients (K) in the D_B models shown in Table 7.1. A calibration of each model is conducted for each representative wave height by gradually adjusting the coefficients of the model pending the error (ER_{avg}) between computed and measured value of each representative wave height was minimum. The calibrated coefficients and the errors of the existing models on simulating H_m, H_{rms}, H_{rmsz}, $H_{1/3}$, and $H_{1/10}$ are shown in Tables 7.2, 7.3, 7.4, 7.5, and 7.6. The results from Tables 7.2, 7.3, 7.4, 7.5, and 7.6 can be summarized in the following points:

a) The coefficients of each model for computing the spectral root-mean-square wave height transformation are smallest and the coefficient of the larger representative wave heights are larger than that of the smaller representative wave heights.

b) With small-scale experiment, most models give excellent accuracy ($ER_{avg} \le 5.0\%$) for computing $H_{1/10}$, give very good accuracy ($5.0\% \le ER_{avg} \le 10\%$) for computing H_{rmsz} (except BJ78 and RS98), and nearly all model give accuracy larger than 10% for computing H_m, H_{rms}, and $H_{1/3}$.

c) With large-scale experiment, most models give very good accuracy ($5.0\% \le ER_{avg} \le 10\%$) for computing $H_{1/10}$ (except AREG08), $H_{1/3}$, H_{rms}, and H_{rmsz}, give good accuracy ($10\% \le ER_{avg} \le 15\%$) for computing H_m (except BHV98, RS08, RS98, RWS03, and MD1 give very good accuracy).

d) With field-scale experiment, most models give very good accuracy ($5.0\% \le ER_{avg} \le 10\%$) for computing H_m (except BHV98), $H_{1/3}$ (except BHV98) and $H_{1/10}$ (except BS85, SN93, BHV98, RS08, and JB07), give good accuracy ($10\% \le ER_{avg} \le 15\%$) for computing H_{rmsz}, and H_{rms} (except MD1).

e) It can be seen from the last column of Table 7.6 that most models (except TG83, SN93, BHV98, and AREG08) give very good overall accuracy. Hence, the parametric wave approach with the calibrated coefficients could be applicable for computing the transformation of H_m, H_{rms}, $H_{1/3}$, $H_{1/10}$, and H_{rmsz}.

f) The models that give the best prediction for H_m, H_{rms}, $H_{1/3}$, $H_{1/10}$, and H_{rmsz} are MD1, MD1, BJ78, BJ78, and BS85 (and JB07), respectively.

g) The average error (ER_{avg}) of the models on computing all H_{rep} in ascending order are MD1, AB07, BS85, RS98, RS08, BJ78, JB07, RWS03, SN93, TG83, BHV98, and AREG08.

h) The average errors of the top four models (MD1, AB07, BS85, and RS98) are 7.6, 8.3, 8.4, and 8.4, respectively. Considering overall accuracy of all models for computing H_m, H_{rms}, $H_{1/3}$, $H_{1/10}$, and H_{rmsz}, the top four models are recommended for calculating transformation of representative wave heights.

Table 7.2 The calibrated coefficients of the collected models for predicting transformation of H_{rep}

Sources	Default coefficients	Calibrated coefficients				
		H_{rmsz}	H_m	H_{rms}	$H_{1/3}$	$H_{1/10}$
BJ78	$K_1 = 0.14$	0.12	0.14	0.14	0.19	0.22
TG83	$K_2 = 0.42$	0.44	0.55	0.60	0.94	0.95
BS85	$K_3 = 0.14$	0.14	0.15	0.16	0.21	0.23
SN93	$K_4 = 1.0$	0.87	1	1.10	1.60	1.70
BHV98	$K_5 = 1.0$	1.00	1.1	1.20	1.50	1.60
RS98	$K_6 = 0.17$	0.1	0.11	0.11	0.17	0.19
RWS03	$K_7 = 0.14$	0.15	0.17	0.17	0.25	0.28
AB07	$K_8 = 0.14$	0.13	0.15	0.16	0.24	0.26
JB07	$K_9 = 1.0$	0.93	1.1	1.10	1.70	1.80
RS08	$K_{10} = 0.14$	0.14	0.15	0.15	0.21	0.23
AREG08	$K_{11} = 1.0$	0.95	1.1	1.30	2.00	2.00
MD1	$K_{12} = 0.14$	0.11	0.12	0.13	0.19	0.22

Table 7.3 The group error of each model for predicting transformation of H_{rep} with the small-scale data by using the calibrated coefficients

Sources	H_m	H_{rms}	$H_{1/3}$	$H_{1/10}$	H_{rmsz}
BJ78	8.6	9.3	9.5	3.3	12.9
TG83	17.2	18.2	17.4	5.0	9.2
BS85	8.1	8.2	10.7	3.7	6.8
SN93	13.9	14.4	16.8	3.9	6.5
BHV98	14.9	16.4	18.1	4.1	7.5
RS98	10.0	9.8	12.8	3.2	12.2
RWS03	15.3	15.1	18.8	4.5	8.7
AB07	7.6	6.9	13.1	2.5	8.0
JB07	12.0	10.7	17.4	3.0	6.7
RS08	9.3	8.2	11.6	3.2	7.2
AREG08	19.7	24.5	23.4	3.9	9.3
MD1	8.3	8.0	9.9	3.9	8.3

Table 7.4 The group error of each model for predicting transformation of H_{rep} with the large-scale data by using the calibrated coefficients

Sources	H_m	H_{rms}	$H_{1/3}$	$H_{1/10}$	H_{rmsz}
BJ78	11.9	6.6	6.1	7.0	8.0
TG83	12.1	6.9	7.6	8.6	8.1
BS85	10.5	6.7	5.8	7.0	6.7
SN93	11.1	6.9	6.7	8.3	7.9
BHV98	9.7	6.8	6.2	7.2	6.5
RS98	8.7	6.4	5.7	6.9	7.1
RWS03	9.9	7.1	6.5	7.7	7.9
AB07	10.6	6.4	7.3	8.9	6.3
JB07	11.7	7.5	7.3	9.5	6.3
RS08	9.4	7.6	5.7	6.9	6.7
AREG08	12.7	7.4	8.0	10.9	9.1
MD1	8.4	6.7	5.9	7.2	6.9

Table 7.5 The group error of each model for predicting transformation of H_{rep} with the field-scale data by using the calibrated coefficients

Sources	H_m	H_{rms}	$H_{1/3}$	$H_{1/10}$	H_{rmsz}
BJ78	5.5	18.9	5.4	5.3	12.6
TG83	5.5	18.4	5.5	6.0	12.6
BS85	8.6	14.2	8.8	10.1	10.5
SN93	9.2	19.8	8.4	10.8	13.4
BHV98	12.3	14.9	12.0	13.5	13.3
RS98	5.7	14.0	5.5	7.0	10.5
RWS03	7.4	15.1	7.2	8.3	10.6
AB07	7.0	14.7	6.6	8.7	10.3
JB07	9.0	13.9	8.6	11.1	10.9
RS08	9.0	13.3	9.0	10.1	10.8
AREG08	6.9	17.9	4.9	6.4	12.2
MD1	7.1	9.7	6.5	6.9	9.6

Table 7.6 The average error of each model for predicting transformation of H_{rep} by using the calibrated coefficients

Sources	H_m	H_{rms}	$H_{1/3}$	$H_{1/10}$	H_{rmsz}	All H_{rep}
BJ78	8.7	11.6	7.0	5.2	11.2	8.7
TG83	11.6	14.5	10.1	6.6	9.9	10.6
BS85	9.0	9.7	8.4	6.9	8.0	8.4
SN93	11.4	13.7	10.6	7.7	9.2	10.5
BHV98	12.3	12.7	12.1	8.3	9.1	10.9
RS98	8.1	10.1	8.0	5.7	9.9	8.4
RWS03	10.8	12.4	10.8	6.8	9.0	10.0
AB07	8.4	9.4	9.0	6.7	8.2	8.3
JB07	10.9	10.7	11.1	7.9	8.0	9.7
RS08	9.2	9.7	8.8	6.7	8.2	8.5
AREG08	13.1	16.6	12.1	7.1	10.2	11.8
MD1	8.0	8.1	7.4	6.0	8.3	7.6

Chapter 8
Conclusions

The present study used laboratory data from 14 resources (total of 1732 cases) including field-scale, large-scale, and small-scale experiment to examine and calibrate parametric wave models, and develop the new model for calculating transformation of representative wave heights. The experiments consist of 2 types of beach conditions, i.e. movable and fixed beach. The data include a wide range of wave and beach conditions. The data consisted of deep-water wave steepness from 0.002 to 0.070.

The new model was developed based on the method of Baldock et.al (1998). Eleven existing models and the present model were examined the possibility for calculating transformation of representative wave heights. The coefficient (K) of each model was calibrated for each representative wave height. Top four models (MD1, AB07, RS98, and BS85 with calibrated coefficients) which give good accuracy were recommended for computing representative wave heights transformation.

References

Alsina, J. M. & Baldock T. E. (2007). Improved representation of breaking wave energy dissipation in parametric wave transformation models. *Coastal Engineering*, 54, 765-769.

Apotsos, A., Raubenheimer, B., Elgar, S. & Guza, R. T. (2008). Testing and calibrating parametric wave transformation models on natural beaches. *Coastal Engineering*, 55, 224-235.

Baldock, T. E., Holmes, P., Bunker, S. & Van Weert, P. (1998). Cross-shore hydrodynamics within an unsaturated surf zone. *Coastal Engineering*, 34 (3-4), 173-196.

Battjes, J. A. & Janssen, J. P. F. M. (1978). Energy loss and set-up due to breaking of random waves. *Proc. 16th Conf. on Coastal Eng., ASCE*, 569-587.

Battjes, J. A. & Stive M. J. F. (1985). Calibration and verification of a dissipation model for random breaking waves. *J. Geophysical Research*, 90 (C5), 9159-9167.

Birkemeier, W.A., Donoghue, C., Long, C.E., Hathaway, K.K., Baron, C.F. (1997). The DELILAH Nearshore Experiment: Summary Data Report. US Army Corps of Engineers, Waterways Experiment Station, Vicksburg, MS.

Dally, W. R., Dean, R. G. & Dalrymple, R. A. (1985). Wave height variation across beach of arbitrary profile. *J. Geophysical Research*. 90(C6), 11917–11927.

Dette, H. H, Peters, K. & Newe, J. (1998). MAST III – SAFE Project: Data Documentation, Large Wave Flume Experiments '96/97, Report No. 825 and 830, Leichtweiss-Institute, Technical University Braunschweig.

Goda, Y. (1970). A synthesis of breaking indices, *Trans. Japan Soc. Civil Eng.* 2,Part 2, 227-230.

Hamilton, D. G. & Ebersole, B. A. (2001). Establishing uniform longshore currents in a large-scale sediment transport facility. *Coastal Engineering*, 42, 199–218.

Herbers, T.H.C., Elgar, S., Guza, R.T., O'Reilly, W.C., (2006). Surface gravity waves and nearshore circulation. DUCK94 Experiment Data Server: SPUV Pressure Sensor Wave Height Data. http://dksrv.usace.army.mi/jg/dk94dirS.

Hotta, S., Mizuguchi, M., Isobe, M. (1982). A field study of waves in the near-shore zone. *18th Coastal Engineering Conference*, 38-57

Hurue, M. (1990). Two-Dimensional Distribution of Undertow due to Irregular Waves. B.Eng. Thesis, Dept. of Civil Eng., Yokohama National University, Japan (in Japanese).

Janssen, T. T. & Battjes, J. A. (2007). A note on wave energy dissipation over steep beaches. *Coastal Engineering*, 54, 711-716.

Katayama, H. (1991). Cross-shore Velocity Distribution due to Breaking of Irregular Waves on a Bar-Type Beach. B. Eng. Thesis, Department of Civil Engineering, Yokohama National University, Japan (in Japanese).

Kraus, N. C. & Smith, J. M. (1994). SUPERTANK Laboratory Data Collection Project. Technical Report CERC-94-3, U.S. Army Corps of Engineers, Waterways Experiment Station, Vol. 1-2.

Le Mehaute (1962). On non-saturated breakers and the wave run-up, *Proc. 8th Coastal Engineering Conf., ASCE*, 77-92.

Nairn, R.B. (1990). Prediction of cross-shore sediment transport and beach profile evolution, *Ph.D. thesis, Dept. of Civil Eng., Imperial College, London*, 391.

Rattanapitikon, W. (2008). Verification of significant wave representation method. *Ocean Engineering*, 35, 1259-1270.

Rattanapitikon, W., Karunchintadit, R. & Shibayama, T. (2003). Irregular wave height transformation using representative wave approach. *Coastal Engineering Journal*, 45, 489-510.

Rattanapitikon, W. & Shibayama T. (1998). Energy dissipation model for regular and irregular breaking waves. *Coastal Engineering Journal*, 40, 327-346.

Rattanapitikon, W. & Sawanggun, S. (2008). Energy dissipation model for a parametric wave approach. *Songklanakarin Journal of Science and Technology*, 30, 333-341.

Rattanapitikon, W. & Shibayama, T. (2010). Energy dissipation model for computing transformation of spectral significant wave height. *Coastal Engineering Journal*, 52, 305-330.

Roelvink, J.A., Reniers, A.J.H.M. (1995). LIP 11D Delta Flume Experiments: A Data Set for Profile Model Validation. Report No. H 2130, Delft Hydraulics.

Ruessink, B. G., Walstra, D. J. R. & Southgate, H. N. (2003). Calibration and verification of a parametric wave model on barred beaches. *Coastal Engineering*, 48, 139-149.

Southgate, H. N. & Nairn, R. B. (1993). Deterministic profile modelling of nearshore processes, Part 1 Waves and currents. *Coastal Engineering*, 19, 27-56.

Smith, J. M. & Kraus, N. C. (1990). Laboratory Study on Macro-features of Wave Breaking over Bars and Artificial Reefs. Technical Report CERC-90-12, U.S. Army Corps of Engineers, Waterways Experiment Station.

Smith, J. M. & Seabergh, W. C. (2001). Wave Breaking on a Current at an Idealized Inlet with an Ebb Shoal, Technical Report ERDC/CHL TR-01-7, Coastal and Hydraulics Laboratory, U.S. Army Engineer Research and Development Center.

Smith, M. K. & Vincent, C. L. (1992). Shoaling and decay of two wave trains on beach. *Journal of Waterway, Port, Coastal, and Ocean Engineering*, 118(5), 517–533.

Thornton, E. B. & Guza, R. T. (1983). Transformation of wave height distribution. *J. Geophysical Research*, 88 (C10), 5925-5938.

Thornton, E.B. and Guza, R.T. (1986). Surf zone long-shore currents and random waves: field data and model. *Journal of Physical Oceanography*. 16, 1165-1178.

Ting, F. C. K. (2001). Laboratory study of wave and turbulence velocity in broad-banded irregular wave surf zone. *Coastal Engineering*, 43, 183-208.